the solvent-casting conditions or other film preparation conditions.[26,52,53]

(50) Shelten, J.; Wignall, G. D.; Ballard, D. G. H.; Longman, G. W. *Polymer* **1977**, *18*, 1111. Wignall, G. D.; Child, H. R.; Samuels, R. J. *Ibid.* **1982**, *23*, 957.

(51) Yang, H.; Hadziioannou, G.; Stein, R. S. *J. Polym. Sci., Polym. Phys. Ed.* **1983**, *21*, 159.

(52) Hasegawa, H.; Yamasaki, K.; Hashimoto, T., to be submitted to *Macromolecules*. Yamasaki, K.; Hasegawa, H.; Hashimoto, T. *Polym. Prepr. Jpn.* **1983**, *32*, 1691.

(53) Hashimoto, T. *Macromolecules* **1982**, *15*, 1548.

(54) In Figure 13, the data in wide q region were purposely shown. It should be noted that the horizontal scale is much more compressed than those used in Figures 11 and 12, resulting in an enhancement of the waviness of the data. If Figure 13 is plotted on the same scale as in Figures 11 and 12, the data fall on the straight lines. The criterion for Guinier's law (eq IV-3) for a homogeneous sphere was stated as $(qR_{gv})^2 \lesssim 1.3^2$ in the text. This criterion is fairly strict; within this criterion the error involved by Guinier's approximation should be less than 4.2% of the rigorous value. If one allows an error of about 15% in the intensity data on the logarithmic scale, the critical value will be much larger: $(qR_{gv})^2 \lesssim 5$; viz., R_{gz} should be obtained from $q^2 \lesssim 0.004$. Although we do not know the exact criterion for the anisotropic system under consideration, we adopted the criterion of $q^2 < 0.004$ to determine R_{gz}.

(55) **Note Added in Proof.** In connection with note 49 above, we have also found that the deuterated block polymer and the protonated block polymer, having different total molecular weights but nearly equal molar compositions, can mix molecularly in a single microdomain morphology. Hasegawa, H.; Hashimoto, T. *Kobunshi Ronbunshu* **1984**, *41*, 759.

Phase Separation in Low Molecular Weight Polymer Mixtures†

Thomas P. Russell* and Georges Hadziioannou

IBM Research Laboratory, San Jose, California 95193

William K. Warburton‡

Stanford Synchrotron Radiation Laboratory, Stanford, California 94304.
Received March 7, 1984

ABSTRACT: The initial stages of phase separation in low molecular weight mixtures of polystyrene (M_w = 2000) and polybutadiene (M_w = 1000 and 2500) have been examined by using time-resolved small-angle X-ray scattering. The high flux from a synchrotron source was utilized due to the rapid kinetics and the weak contrast at the early stages of phase separation. Over the scattering vector range studied (from q = 0.07 to 0.97 nm^{-1}) no evidence of a scattering maximum, characteristic of a periodic variation in the concentration, was observed. At the onset of phase separation, the intensity at a constant scattering vector was found to depend exponentially on time with an amplification factor $R(q)$ that changed from positive values at low q to negative values at high q. According to the Cahn-Hilliard theory,[1,2] these crossover points were used to estimate the spinodal temperatures and Flory-Huggins interaction parameters. Deviations of the scattering vector dependence of $R(q)$ strongly suggest that thermal density fluctuations not taken into account by the Cahn-Hilliard theory contribute significantly to the observed scattering.

Introduction

The kinetics of phase separation in polymer mixitures is not yet understood quantitatively. In contrast to the numerous theoretical and experimental treatments of this problem (see, for example: ref 3 and 4) for small molecular mixtures, the polymeric analogues have received relatively little attention. de Gennes[5] and, later, Pincus[6] have attempted to theoretically treat the kinetics of demixing in bulk polymer mixtures by modifying the existing Cahn-Hilliard theory.[1,2] Experimentally, Bank, Leffingwell, and Thies[7] first observed the reversible phase separation of high molecular weight polymer mixtures in the polystyrene (PS)/poly(vinyl methyl ether) (PVME) system using differential scanning calorimetry and dielectric relaxation. Subsequent to this, Nishi, Wang, and Kwei[8] using both optical microscopy and NMR[5] first examined the kinetics of phase separation in this mixture. From their studies, they concluded that the phase separation process could be adequately described in terms of the Cahn-Hilliard model. Gelles and Frank,[9] utilizing excimer fluorescence to probe the changes in local concentration as a function of time, confirmed these findings. Recently, Hashimoto and co-workers[10] extended studies on this mixture by small-angle light scattering (SALS) and quantitatively interpreted their results using the de Gennes-Pincus modification to the Cahn-Hilliard theory. On this same system, Snyder et al.[11,12] performed an extensive series of measurements using SALS. In contrast with previous work, they found that only the very early stages of phase separation could be described by the linearized theories. Incorporation of nonlinear terms was necessary in order to fully describe the process and, it may be argued, that the agreement between experiment and linearized theories was fortuitous.

While other polymer mixtures are known to possess lower critical solution temperatures (LCST) the LCST of PS/PVME conveniently occurs at temperatures well above the glass transition temperature and much lower than the decomposition temperature of either component. Consequently, there is little information available on the kinetics of phase separation for other high molecular weight polymer mixtures.

Phase separation in lower molecular weight polymer mixtures has been studied by Nojima and co-workers[13-16] using SALS. Mixtures of PS with poly(methylphenylsiloxane) (PMPS) were found to exhibit upper critical solution temperature (UCST) behavior. As expected, the rates of the phase separation were more rapid than with the higher molecular weight mixtures. However, they did not find agreement with the Cahn-Hilliard theory and required the nonlinear treatments[17-19] in order to quan-

† Some of the materials incorporated in this work were developed at SSRL with the financial support of the National Science Foundation (Contract DMR77-27489) (in cooperation with the Department of Energy).

‡ Present address: University of Southern California, Marina DelRey, CA 90292.

0024-9297/85/2218-0078$01.50/0

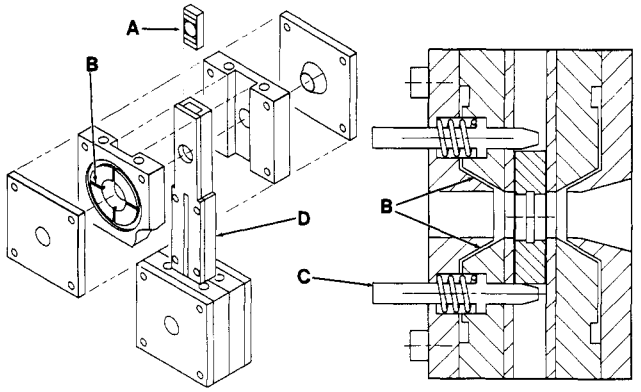

Figure 1. Perspective drawing of the double-furnace sample holder (left) with a vertical cross section of furnace shown in detail (right). An explanation of the important features is given in the text.

titatively interpret their results.

Optical techniques have been the dominant means of probing the development and growth of periodic concentration fluctuations in polymer mixtures undergoing phase separation. Due to the wavelength of light (>400 nm), SALS is restricted to dimensions on the order of microns which is many times larger than the individual molecules in the mixture. Clearly, substantial changes have occurred in the mixture on a size scale where SALS is not sensitive. In this paper, the kinetics at the early stages of phase separation are investigated by using time-resolved small-angle X-ray scattering (SAXS) which probes concentration or electron density correlations up to several tens of nanometers. It is the intent of this study to examine the applicability of the linearized theory of spinodal phase separation to polymer mixtures on this small size scale. This study addresses low molecular weight mixtures, which avoids the question of entanglements and enhances the possibility at examining the linear approximations over a larger time scale.

Experimental Section

The desired weight of PS (M_w = 2000, M_w/M_n = 1.3) was added directly to a preweighed quantity of PBD (M_w = 1000, M_w/M_n = 1.2, and M_w = 2500, M_w/M_n = 1.15). Stirring these bulk mixtures at 130 °C for 5 min under nitrogen produced a homogeneous fluid that was transferred to the scattering cells with a preheated Pasteur pipette. The scattering cells consisted of two interconnecting stainless steel rings (1 mm in thickness with inner and outer diameters of 4.7 and 6.4 mm, respectively) with 13-μm Kapton windows. A chromen-alumel thermocouple was placed directly within the mixtures via 0.025-mm diameter holes in the rings.

The heating chamber used in the SAXS measurements is shown in Figure 1. The sample cell, supported in carriage A, was held by spring loaded pins within the upper oven. Preheated helium passed over both surfaces of the specimen via small conduits within the heating block B in order to improve heat transfer to the specimen. The sample was quenched by releasing the lower pin, allowing it to fall within track D onto a locating pin that centered the sample in the window of the lower oven. The lower oven was centered about the incident X-ray beam via micrometers on a support stage. Thermal equilibration of the specimen was attained within 5–10 s.

During the initial stages of phase separation, the contrast or electron density difference is small. Coupling this with the rapid rate of phase separation mandated the use of a high-flux source and a high-speed detector. Consequently, the SAXS facility on BL I-4 at the Stanford Synchrotron Radiation Laboratory (SSRL) was utilized in this study.

A detailed description of the SAXS facility at SSRL has been reported elsewhere.[20] Briefly, the beam from the storage ring is focused vertically by a 1.25-m float glass mirror and horizontally by an asymmetrically cut silicon crystal to a point several centimeters before the beamstop. At the detector, the measured half-widths of the beam were 0.15 and 0.44 mm in the vertical and horizontal directions, respectively. The wavelength of the X-ray was determined to be 0.1412 nm with an energy resolution, $\Delta E/E$, of 7×10^{-3}. The total intensity of the focused beam has been measured at 2.6×10^9 cps at the detector with the storage ring operating at 85 ma and 3.0 GeV. Due to the gradual reduction of current in the storage ring after beam injection, the incident intensity was constantly monitored with a detector immediately before the specimen. In addition, a monitor positioned directly after the specimens provided the attenuation factor of the specimen. SAXS profiles from 0.07 to 0.97 nm^{-1} were collected with a detector system consisting of a 1024 pixel self-scanning photodiode array. The minimum time required to acquire and store the data was approximately 0.5 s. The effective dimensions of each photodiode were 2.0 and 0.025 mm in the horizontal and vertical directions, respectively. All scattering profiles were corrected for detector homogeneity, electronic noise, and parasitic scattering in the standard fashion.

Since the detector elements were wider than the beam in the horizontal direction, a smearing of the experimentally obtained data from the detector resulted. Convolution of the horizontal beam profile with the shape function of a detector element yielded the slit length weighting function.[21] To within experimental errors, this could be approximated by a trapezoid. Consequently, a modified version of the desmearing routine developed by Strobl[22] was used to correct each scattering curve.

Theoretical Background

The free energy, f, for an unstable mixture at the initial stage of phase separation can be written as

$$f = \int [f_0 + \kappa(\nabla c)^2 + ...]\, dv \tag{1}$$

where f_0 is the free energy density of the homogeneous mixture and $\kappa(\nabla c)^2$ is an additional contribution to the free energy density arising from concentration gradients. Solving a modified diffusion equation, Cahn[1] has shown that the rate at which the concentration at a position r will change from its initial value, c_0, is given by

$$c(r,t) - c_0 = (1/2\pi)^3 \int A(q,t) e^{-iqr}\, dq \tag{2}$$

where q is the wave number of the fluctuations in Fourier space. $A(q,t)$ is the amplitude of the fluctuation and is related to the initial amplitude at time $t = 0$ by

$$A(q,t) = A(q,0) e^{R(q)t} \tag{3}$$

where $R(q)$ is the amplification factor defined by

$$R(q) = -M(\partial^2 f/\partial c^2)q^2 - 2M\kappa q^4 \tag{4}$$

where M is the mobility. $R(q)$ has a maximum value at $q = q_m$ where

$$q_m^2 = -(\partial^2 f/\partial c^2)/4\kappa \tag{5}$$

and $R(q)$ is zero at $q = q_c$ where

$$q_c^2 = -(\partial^2 f/\partial c^2)/2\kappa \tag{6}$$

For values of $q < q_c$, i.e., for fluctuation larger than the critical value, $R(q)$ is positive and the fluctuations grow in time, while for $q > q_c$, $R(q) < 0$ and the fluctuations will decay with time.

Since the electron density is proportional to the concentration, the amplitude of scattering, $B(q,t)$ will be related to the Fourier transform of the concentration fluctuation

$$B(q,t) \propto \int (c,(r,t) - c_0) e^{-iqr}\, dr \tag{7}$$

Consequently, the intensity of scattering is given by

$$I(q,t) = I(q,0) e^{2R(q)t} \tag{8}$$

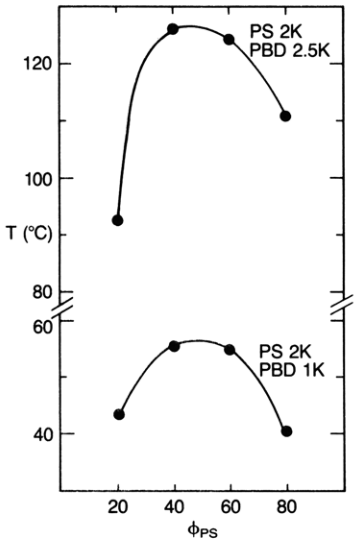

Figure 2. Cloud point curves for mixtures of PS(M_w = 2000) with PBD(M_w = 2500 (upper) and M_w = 1000 (lower)) as determined from optical density measurements.

Using a modified Flory–Huggins free energy of mixing, de Gennes[5] determined the free energy of a polymeric mixture undergoing spinodal phase separation to be

$$\frac{f}{kT} = \frac{\phi_A}{N_A} \ln \phi_A + \frac{\phi_B}{N_B} \ln \phi_B + \phi_A\phi_B\chi + \frac{a^2}{36\phi_A\phi_B}(\nabla c)^2 \tag{9}$$

where ϕ_A is the volume fraction of component A with degree of polymerization N_A, χ is the Flory–Huggins interaction parameter and a is the Kuhn segment length assumed to be same for both components. Using the continuity equation and relating the local current of one component to the chemical potential, via the Onsager coefficient, $\Lambda(q)$, the amplification factor was shown to be given by

$$R(q) = -q^2\Lambda(q)\left[\frac{1}{N\phi_A\phi_B} - 2\chi + \frac{(aq)^2}{36\phi_A\phi_B}\right] \tag{10}$$

where $N_A = N_B = N$. Subsequently, Pincus[6] evaluated $\Lambda(q)$ for high molecular weight polymer mixtures by using reptation arguments and found that $\Lambda(q) \sim q^{-2}$. However, due to the molecular weights used in this study, reptation should not be applicable and $\Lambda(q)$ should be a constant independent of q as in small molecule systems.

Results and Discussion

The cloud point curves (CPC) for the PS/PBD mixtures determined from optical density measurements at several heating and cooling rates and extrapolated to an infinitely slow rate of temperature change are shown in Figure 2. As expected, the CPC occurred at higher temperatures as the molecular weight was increased. The CPC's represent the binodal line for the mixtures where, at equilibrium, phase separation would occur. Since the location of the spinodal line was unknown, the time-resolved SAXS was examined at several different temperatures at each concentration studied. Prior to each measurements, the mixtures were homogenized by heating to at least 25 °C above the binodal.

Two different examples of time-resolved SAXS profiles obtained every 1.25 s are shown in Figure 3a for a 60% PS(2K)/40% PBD(1K) mixture quenched to 42 °C and Figure 3b for an 80% PS(2K)/20% PBD(2.5K) mixture quenched to 105 °C. The first profile in each series corresponds to the time when thermal equilibrium was obtained. This required discarding the first 5–8 profiles recorded during the quench. A time of t = 0 was set when the mixtures had attained thermal equilibrium. Absolute determination of t = 0 was not necessary for the analysis.

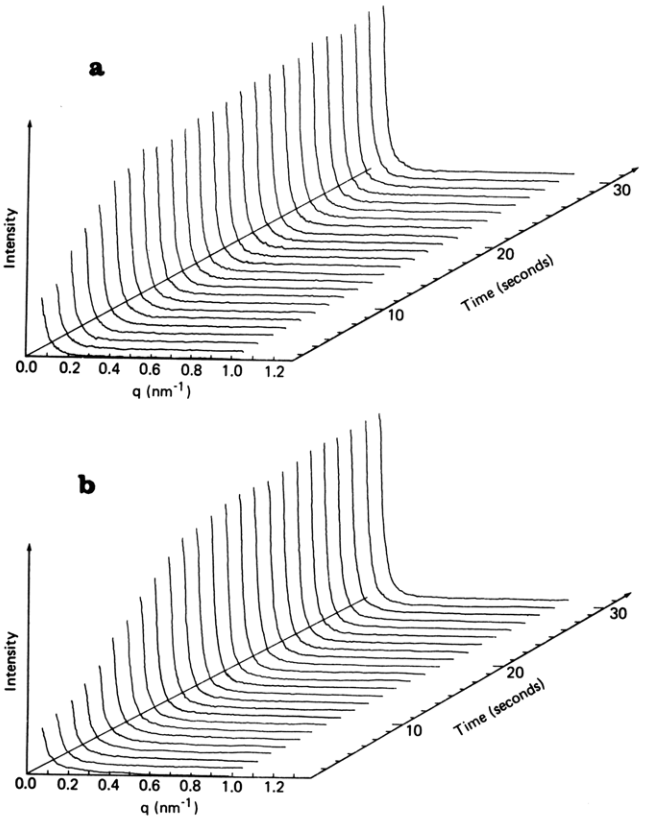

Figure 3. (a) Time-resolved SAXS for a 60% PS(2K) with 40% PBD(1K) quenched to 42 °C at 1.25-s time intervals. (b) Time-resolved SAXS for an 80% PS(2K) with 20% PBD(2.5K) quenched to 105 °C at 1.25-s time intervals.

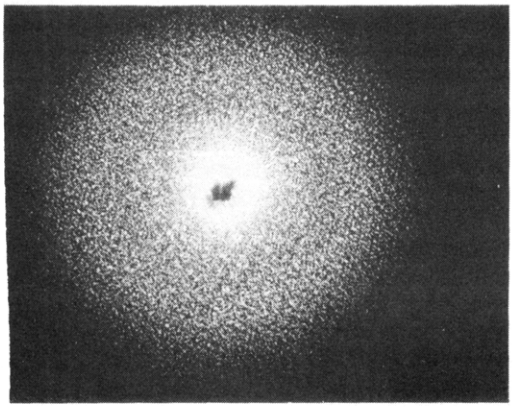

Figure 4. Small-angle light scattering pattern for a 50% PS(2K)/50% PBD(2.5K) quenched to room temperature for several minutes. The maximum corresponds to ca. 1.5 μm.

A dramatic increase in the SAXS at low q was observed during the first minute of phase separation. In addition, from q = 0.07 to 0.97 nm^{-1}, no evidence of a scattering maximum was found. This was found to be the case for all the mixtures investigated regardless of the quench depth. It is apparent that, if the mixtures are undergoing spinodal phase separation, the characteristic wavelength describing a periodic concentration modulation is much larger than 80 nm. This result contrasts the typical results found by SALS where a scattering maximum is clearly evident. An example of such a pattern is shown in Figure

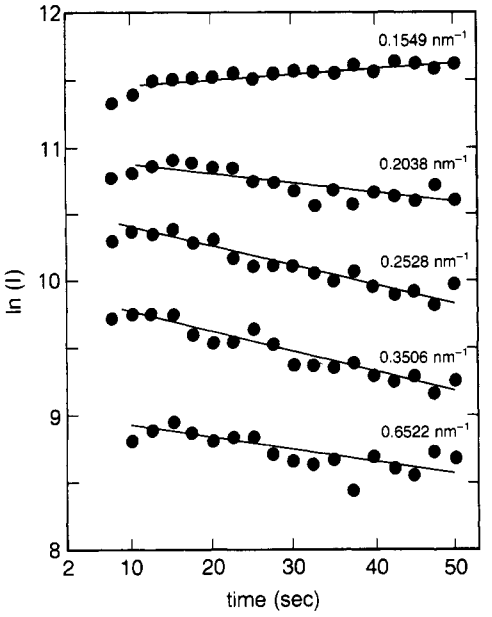

Figure 5. Ln (I) vs. t for a 60% PS(2K)/40% PBD(1K) quenched to 42 °C. The values of q shown are samples from the q range studied.

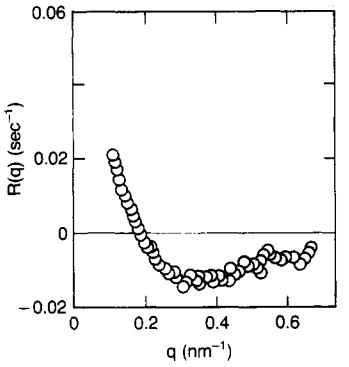

Figure 6. Amplification factor, $R(q)$, as a function of q for a 50% PS(2K)/40% PBD(1K) quenched to 42 °C. The errors of each $R(q)$ are well within the size of points.

4 which clearly shows a maximum occurring at a Bragg spacing corresponding to 1.5 μm. The diffuse appearance of the pattern is due to the sample thickness and the late stages, i.e., long time (ca. 3 min), at which the photograph was taken. In comparison to the radii of gyration of the individual components (ca. 3 nm) it is clear that the morphological changes occur on a size scale many times the molecular dimensions. Consequently, the formation of a periodic concentration fluctuation involves a long range cooperativity of the individual molecules.

In order to define the phase separation in terms of a nucleation and growth or a spinodal mechanism, the rate of change for the intensity at individual values of q was examined. The log of the intensity as a function of time is shown in Figure 5 for a 60% PS(2K)/40% PBD(1K) mixture. Approximate linear behavior was found at early times. This is consistent with the predictions of the Cahn–Hilliard theory where the intensity is predicted to change exponentially with time. The slopes of the lines in Figure 5 yield the amplification factors, $R(q)$, defined in eq 4 and 8. A systematic change in the sign and magnitude of $R(q)$ are evident. Plotting $R(q)$ as a function of q in Figure 6 show a distinct crossover point, q_c, where $R(q) = 0$. Values of q_c determined for the various mixtures investigated are given in Table I along with the corresponding quench temperature. In addition to q_c, a minimum in $R(q)$ was observed.

Table I
Results for PBD Mixtures with PS(2K)

M_w(PBD)	ϕ_{PS}	T,[a] °C	q_c, nm^{-1}	χ	T_s, °C
1000	0.4	35	0.210	0.110	53
	0.4	40	0.169	0.111	
	0.4	42	0.153	0.111	
	0.4	45	0.145	0.110	
	0.6	40	0.180	0.110	
2500	0.2	82	0.334	0.073	89
	0.2	84	0.295	0.073	
	0.2	85	0.294	0.073	
	0.2	85	0.251	0.073	
	0.4	110	0.163	0.059	
	0.6	112	0.195	0.069	
	0.8	104	0.316	0.126	114
	0.8	105	0.288	0.127	
	0.8	105	0.283	0.127	
	0.8	105	0.279	0.128	

[a] Quench temperature.

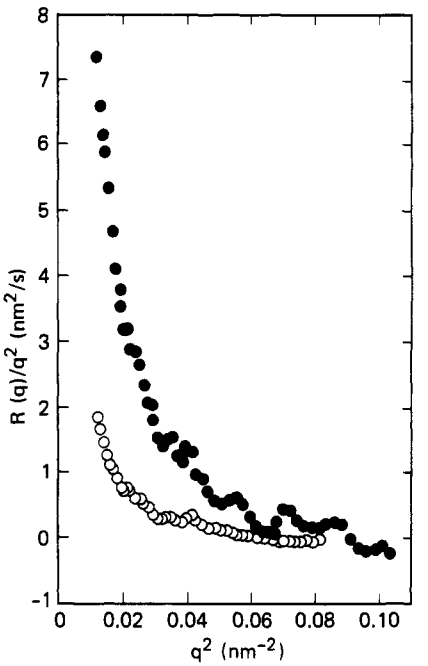

Figure 7. $R(q)/q^2$ vs. q^2 for an 80% PS(2K)/20% PBD(2.5K) quenched to 104 °C (●) and 105 °C (○).

From eq 5 and 6, q_c is related to the q_m, the value of q where $R(q)$ is a maximum, by a factor of $2.^{1/2}$ Calculated values of q_m are all greater than 0.115 nm^{-1}. Therefore, according to eq 8, a maximum in the scattering profiles should be observed at Bragg spacings less than 63 nm which was well within the resolution of the instrument. As mentioned previously, this was not observed and demonstrates an inadequacy of eq 4. It should be noted that q_m^2/q_c^2 in higher molecular weight mixtures,[23] as well as in metallic alloys[24,25] has been found to be significantly smaller than the predicted 1/2 which is consistent with the results obtained in this study.

The discrepancy between q_c and q_m is most likely due to shortcomings in the classical definition of $R(q)$. This is magnified when the q dependence of $R(q)$ is examined. $R(q)/q^2$ according to eq 4 should depend linearly upon q^2. As shown in Figure 7, for two different quenches of an 80% PS(2K)/20% PBD(2.5K) mixture, significant curvature was found. Determination of an apparent diffusion coefficient, D_{app}, from $R(q)/q^2|_{q=0}$ was ambiguous. When only the low q^2 part of Figure 7 was used, D_{app} increased with lower quenching temperatures, as would be expected;

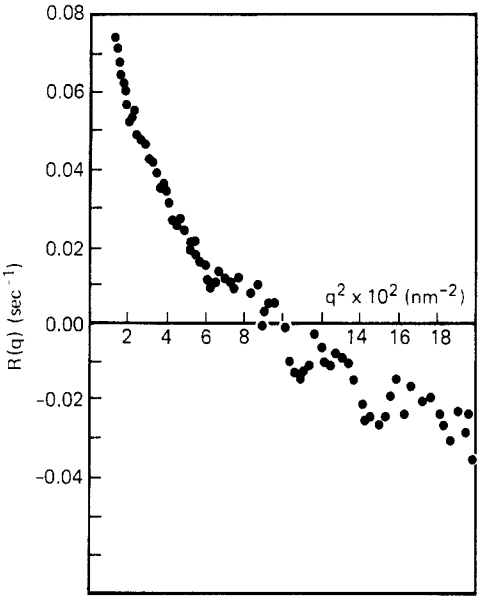

Figure 8. $R(q)$ vs. q^2 for an 80% PS(2K)/20% PBD(2.5K) quenched to 105 °C.

however, unrealistically low values were found.

One possible origin for the disagreement between the experiments and the classical linearized theories is the neglect of higher order terms in the Taylor expansion of the concentration gradient. In a mean field pair interaction analysis, Uhlmann and Hopper[26] circumvented this problem by using a Fourier expansion to describe the concentration gradient, thereby, including all higher order terms. Equation 4, according to their analysis, becomes

$$R(q) = -M(\partial^2 f/\partial c^2)q^2 - Mq^2\kappa(q) \tag{11}$$

The dependence of $\kappa(q)$ on q, as discussed by these authors, depends strongly upon the intermolecular potentials used. In the limit of small q, $\kappa(q)q^2$ approaches κq^4, the classical result. At large, q, $\kappa(q)$ was independent of q, suggesting that $R(q)$ should depend upon q^2. While the curvature exhibited in Figure 8 is less marked than that in Figure 7 deviations from linearity are clearly evident at higher q.

The failure of the Cahn–Hilliard theory to accurately predict the q dependence of $R(q)$ has also been observed in metallic alloys.[27-29] Cook[30] and others[31] have argued that the major inadequacy of the Cahn–Hilliard theory is not associated with the linear approximations but rather with the omission of a term due to fluctuation scattering of a stable solution. According to eq 8 at $t = \infty$, the scattered intensity would vanish. In order to circumvent this, Cook introduced a term, $L(q,\infty)$ into eq 8 due to the scattering arising from pair correlations present in the mixture at equilibrium. At low q, $L(q,\infty)$ is identical with the Orstein–Zernicke function and is given by

$$L(q,\infty) = \frac{kT}{\phi(1-\phi)\Omega((\partial^2 f/\partial c^2) + 2\kappa q^2)} \tag{12}$$

where Ω is the volume per monomer unit. Incorporation of this into the Cahn–Hilliard theory yields a scattered intensity that is given by

$$I(q,t) = (I(q,0) - L(q,\infty))e^{2R(q)t} + L(q,\infty) \tag{13}$$

Quantitative use of eq 13 is difficult since $L(q,\infty)$ must be approximated from the experimental data. However, there are several important ramifications that arise from Cook's modification. First, the value of $R(q)$ determined according to eq 8 would not be correct. From eq 13 plots of ln $(I(q,t))$ vs. t should not be linear but exhibit curvature. This is evident in Figure 5 as well as in other published data.[10,12] Second, values of q_c are identical in both theories since this is independent of the manner in which $R(q)$ was determined. Third, the minimum in $R(q)$ observed at high values of q would be attributable to the contributions to $I(q,t)$ from $L(q)$. Since $L(q)$ is independent of time, it would tend to reduce variations in the observed intensity in a region where the scattering is inherently weak. In addition, the ratio of $(q_m/q_c)^2$ is not predicted to be $^1/_2$ but is given by[30]

$$\left(\frac{q_m}{q_c}\right)^2 = \frac{T_s - T_a}{2T_s} \tag{14}$$

where T_s and T_a are the spinodal and quench temperatures, respectively. Only when $T_a = 0$ K would a value of $^1/_2$ be expected. Under normal experimental conditions, the ratio would be less than $^1/_2$, which would account for the absence of a scattering maximum in this study. Finally, quenching to below the spinodal temperature is not necessary to observe a crossover point. In fact, quenching a homogeneous mixture from one temperature to another but remaining in the single phase, miscible region would produce a crossover point. This crossover point, not predicted by Cahn–Hilliard theory, arises from the intersection of two different Ornstein–Zernicke functions.

Since q_c is not affected by the manner in which $R(q)$ was determined and is only a function of the thermodynamics of the phase separating mixture, eq 10 was used to evaluate the Flory–Huggins interaction parameter, χ. R_0^2, the mean square end-to-end distance, is given by Na^2 and $\chi_s = 1/(2N\phi_A\phi_B)$; then at $q = q_c$ from eq 10 we get

$$\chi = \chi_s(1 + q_c^2R_0^2/36) \tag{15}$$

Values of χ calculated from eq 15 using an average value of R_0 for the two components are given in Table I. χ was found to be positive in all cases which is reasonable for a polymer mixture undergoing phase separation. In all cases, however, χ was dominated by χ_s since $q_c^2R_0^2/36 \ll 1$.

Equation 10 can also be solved for q_c, yielding

$$q_c^2 = \frac{36}{R_0^2}\left(\frac{\chi_s - \chi}{\chi_s}\right) \tag{16}$$

which near the spinodal temperature can be rewritten as

$$q_c^2 = \frac{36}{R_0^2}(T_s - T) \tag{17}$$

The temperature dependence of q_c^2 is shown in Figure 9. The intercept of $q_c = 0$ yielded the spinodal temperature. T_s for several mixtures is shown in Table I. Unfortunately, the precision to which T_s could be determined was low due to the limited range of quench temperatures near T_s. According to eq 15, q_c should also depend upon N^{-1}. However, from the data in Table I and from the results of Snyder and Meakin,[31] q_c is found to increase with increasing N.

Recently, Ronca and Russell[32] reexamined the thermodynamics of phase separating polymer mixtures. Using a bead/spring model for a polymer chain within a concentration gradient that is much larger than the size of the individual molecules and assuming a temperature dependent χ, they found that the critical fluctuation wavenumber or crossover point, q_c, depended upon χ and N. This dramatically differs from the previous predictions but is consistent with this work and that of Snyder and Meakin.[31]

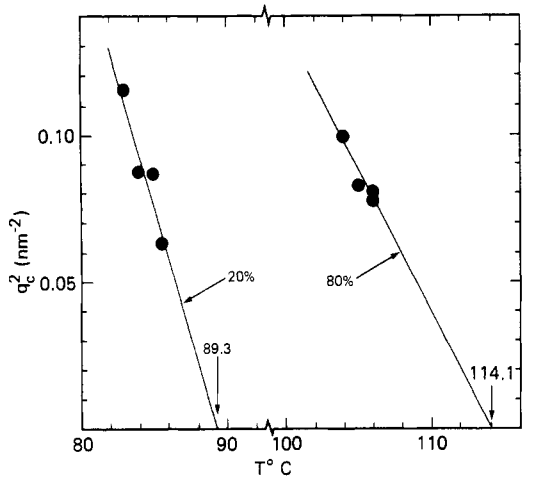

Figure 9. Square of the crossover point, q_c^2, as a function of temperature for an 80% and 20% mixture of PS(2K) with PBD(2.5K).

Conclusion

The initial stages of phase separation in low molecular weight mixtures of polystyrene with polybutadienes have been investigated by means of time-resolved small-angle X-ray scattering. The results presented only qualitatively agree with the classical theory of spinodal phase separation developed by Cahn and Hilliard. The data indicated that an additional contribution to the scattering equivalent to the Ornstein–Zernicke scattering from a homogeneous mixture at equilibrium was necessary in order to fully describe the scattering. A critical wavelength, q_c, was observed where the rate of intensity change was zero. This was used to evaluate the Flory–Huggins interaction parameter for the different mixtures. q_c^2 was found to vary linearly with the temperature and permitted the evaluation of the spinodal temperature. In addition, q_c was found to increase with an increase in the molecular weight of one of the components.

Acknowledgment. It is a pleasure to acknowledge J. Cockerill, R. Bucher, and J. Buchanan of Central Scientific Services at IBM for their assistance in the design and construction of the sample cell. We are also grateful to D. Quilici for her assistance in the sample preparation. We also thank D. Sosa and R. Hwang of the User Services Group who made the transfer of data from SSRL to IBM possible. Finally, fruitful discussions with G. B. Stephenson (IBM, Yorktown) and G. Ronca (IBM, San Jose) were greatly appreciated.

Registry No. PS (homopolymer), 9003-53-6; PBD (homopolymer), 9003-17-2.

References and Notes

(1) Cahn, J. W. *Trans. Metall. Soc. AIME* **1968**, *242*, 166.
(2) Hilliard, J. E. "Phase Transformations"; Aronson, H. I., Ed.; American Society for Metals: Metals Park, OH, 1967.
(3) Goldburg, W. I. "Scattering Techniques Applied to Supramolecular and Nonequilibrium Systems"; Chen, S., Chu, B., Nossal, R., Eds.; Plenum Press: New York, 1980; p 383.
(4) Langer, J. S. "Fluctuations, Instabilities, and Phase Transitions"; Riste, T., Ed.; Plenum Press: New York, 1975; p 19.
(5) de Gennes, P.-G. *J. Chem. Phys.* **1980**, *72*, 4756.
(6) Pincus, P. *J. Chem. Phys.* **1981**, *75*, 1996.
(7) Bank, M.; Leffingwell, J.; Thies, C. *J. Polym. Sci., Part A-2* **1972**, *10*, 1097.
(8) Nishi, T.; Wang, T. T.; Kwei, T. K. *Macromolecules* **1975**, *8*, 227.
(9) Gelles, R.; Frank, C. W. *Macromolecules* **1982**, *15*, 1486.
(10) Hashimoto, T.; Kumaki, J.; Kawai, H. *Macromolecules* **1983**, *16*, 641.
(11) Snyder, H. L.; Meakin, P.; Reich, S. *J. Chem. Phys.* **1983**, *78*, 334.
(12) Snyder, H. L.; Meakin, P.; Reich, S. *Macromolecules* **1983**, *16*, 757.
(13) Nojima, S.; Tsusumi, T.; Nose, T. *Polym. J.* **1982**, *14*, 225.
(14) Nojima, S.; Nose, T. *Polym. J.* **1982**, *14*, 269.
(15) Nojima, S.; Ohyama, Y.; Yamaguchi, M.; Nose, T. *Polym. J.* **1982**, *14*, 907.
(16) Nojima, S.; Shiroshita, K.; Nose, T. *Polym. J.* **1982**, *14*, 289.
(17) Langer, J. S.; Bar-on, M.; Miller, H. D. *Phys. Rev. A* **1975**, *A11*, 1417.
(18) Binder, K.; Stauffer, D. *Phys. Rev. Lett.* **1974**, *33*, 1006.
(19) Kawasaki, K.; Ohta, T. *Prog. Theor. Phys.* **1978**, *59*, 362.
(20) Stephenson, G. B. Ph.D. Thesis, Department of Material Science and Engineering, Stanford University, 1982.
(21) Gerold, V. *Acta Crystallogr.* **1975**, *10*, 287.
(22) Strobl, G. *Acta Crystallogr., Sect. A* **1970**, *A26*, 367.
(23) Snyder, H. L., private communication, 1983.
(24) Agarwal, S.; Herman, H. *Scr. Metall.* **1973**, *7*, 503.
(25) Acuna, R.; Bonfiglioni, A. *Acta Metall.* **1974**, *22*, 399.
(26) Hopper, R. W.; Uhlmann, D. R. *Acta Metall.* **1973**, *21*, 35, 377.
(27) Rundman, K. B.; Hilliard, J. E. *Acta Metall.* **1967**, *15*, 1025.
(28) Hilliard, J. E. "Phase Transformations"; Aaronson, H. I., Ed.; American Society for Metals: Metals Park, OH, 1970; p 497.
(29) Cook, H. E. *Acta Metall.* **1970**, *18*, 297.
(30) Park, M. W.; Cooper, A. R.; Hener, A. H. *Scr. Metall.* **1975**, *9*, 32.
(31) Snyder, H. L.; Meakin, P. *J. Polym. Sci., Macromol. Rev.*, in press.
(32) Ronca, G.; Russell, T. P. *Macromolecules*, in press.

Phase Transition in Ionic Gels Induced by Copper Complexation

J. Rička and T. Tanaka*

Department of Physics and Center for Materials Science and Engineering, Massachusetts Institute of Technology, Cambridge, Massachusetts 02139. *Received May 23, 1984*

ABSTRACT: Acrylic acid–acrylamide copolymer gels immersed in water solutions of Cu(II) salts exhibit a discontinuous volume collapse upon continuous increase of Cu(II) concentration. The phenomenon, which occurs when the acrylic acid content of the gel exceeds a certain critical value, is attributed to formation of Cu(II) complexes with ligands attached to the network. A qualitative description of the phenomenon, based on an analogy between the formation of complexes in a copper salt solution and the formation of energetically favorable contacts between polymer segments in a poor solvent, is presented.

Introduction

In a previous study[1] we investigated the swelling of acrylic acid–acrylamide copolymer gels in water solutions of several simple electrolytes, focusing our attention on salts of alkali metals and alkaline-earth metals. When only monovalent ions are involved, the observed swelling is in good quantitative agreement with the predictions of the simple Donnan equilibrium theory. In the presence of

0024-9297/85/2218-0083$01.50/0